Rotorcraft Multi-Objective Trajectory Optimization for Low Noise Landing Procedures

Luís Cruz
Aeroacoustics Engineer
CEIIA, Aerodynamics Dept
luis.cruz@agustawestland.com

Andrea Massaro
Aerodynamics Specialist
AgustaWestland, Aerodynamics Dept.
andrea.massaro@agustawestland.com

Stefano Melone
Aerodynamics Specialist
AgustaWestland, Aerodynamics Dept.
stefano.melone@agustawestland.com

Andrea D'Andrea[1]
Rotor Aerodynamics Technical Leader
AgustaWestland, Aerodynamics Dept.
andrea.dandrea@agustawestland.com

ABSTRACT

An advanced optimization procedure was developed to allow the calculation of reduced noise approach trajectories by employing the latest advances in the fields of rotorcraft aerodynamic and acoustic simulations, coupled with an efficient multi-objective automatic optimization algorithm. The computational chain put in place is able to quickly optimize for low noise the approach trajectory of any rotorcraft configuration and at the same time respect the operational and passenger comfort restrictions. In this work one conventional helicopter was analyzed with the results of the optimized trajectories being compared to a standard approach path. The optimized approach procedures are predicted to significantly reduce the on-ground noise.

NOTATION

BVI	Blade Vortex Interaction
MR	Main Rotor
TR	Tail Rotor
OASPL	Overall Sound Pressure Level [dB][dBA]
SEL	Sound Exposure Level [dBA]
VRS	Vortex Ring State

INTRODUCTION

Rotorcrafts are easily recognised by their characteristic rotor noise which is also why sometimes they are considered a source of great annoyance. The noise of the rotors is mostly dominated by the tonal components in the approach phase, often the most critical one in terms of generated and perceived noise, as it involves operations close to the ground and near or above populated areas. There are several ways to minimize the rotor noise, either using rotor technologies (passive or active) or using landing procedures that minimize the on-ground noise by avoiding the Blade Vortex Interaction (BVI) region. Rotor technologies often require a (costly) redesign of the rotor blade and hub to fully take advantage of the benefits provided by it and retrofitting it to legacy helicopters is often not feasible, whereas using new landing procedures, tailored to any helicopter, would simply require a (less costly) avionics upgrade and pilot training. With this in mind, AgustaWestland has been spending a lot of effort dedicated to the study of "green" operations. In particular, the optimization of flight paths for helicopter silent operations near populated areas and the associated operational requirements are at present under investigation.

STATE-OF-ART

Le Luc et al [1] present a study where an hybrid computational chain is used to predict the noise footprint on-ground of an helicopter in "arbitrary" flight. That includes an acoustic database obtained experimentally during several flight tests and that was used to create several hemispheres along with a numerical characterization of the helicopter based on a few aerodynamic parameters and a numerical propagation of the hemispheres down to the ground. Since the acoustic database was obtained experimentally all the noise sources are present, although for typical approaches the Main Rotor harmonics normally dominate. Because not all the

[1] Corresponding author

relevant aerodynamic parameters (e.g. main rotor angle of attack) were obtained during the experimental trials, a flight mechanics tool was used to predict those based on the other acquired data. The simulated flight paths have their position and velocity described by cubic Bezier curves. These paths were rejected if they didn't meet the comfort and flyability criteria, in particular having high accelerations, VRS, certain regions of the H-V diagram and autorotation. The whole computational chain was validated against the available experimental data and a good matching was obtained for the SPL. This tool was then coupled with an optimizer and validated under the framework of the Friendcopter EU research project [2][3]. It was concluded that torque can be a good parameter as a BVI avoidance indicator. Intermediate torque regions were found to be noisy whereas the low and high torque regions were found to avoid BVI. Since the studied helicopter was the EC135, it was also found that the annoying Fenestron noise could be avoided by sidesliping the helicopter. Regarding the optimization studies, it was concluded that the optimized flight paths were relatively insensible to side wind and helicopter mass variations while headwind was found to have a noticeable impact. Several flight paths were tested, with flight testing confirming the predicted 10[dBA] reduction in SEL between 1 and 3[km] before the landing point.

A fully numerical computation chain was developed by Perez et al [4] to analyse low noise flight procedures by coupling helicopter trim, aerodynamics and acoustics tools. This numerical chain included tools initially developed for steady conditions but were improved to analyze transient manoeuvres. The work was focused on MR noise, namely BVI noise reduction in descent and entry in a turn. For the descent case it was concluded that the peak level of noise was reduced by 20[dB] thanks to the deceleration effect on the rotor angle of attack. Flight testing confirmed that the Main Rotor BVI disappeared but the observed gains were only up to 6[dB] as the other noise sources became more important than the Main Rotor noise.

The work of Ikaida et al [5][6] was focused on developing a real time trajectory optimization based on numerical simulations. The optimization algorithm used was the Direct Collocation with Non-Linear Programming with Sparse Sequential-Quadratic-Programming. The noise source model had to be simple enough to allow real time calculations so the noise data obtained from flight experiments was reduced to simple equations. These equations had a modified flight path angle that took into consideration the effect of accelerating/decelerating helicopter, as this has a very big effect on the rotor tip path plane angle of attack and, consequently, the occurrence of BVI. In addition, a Performance Index model was included by referring to a sound exposure level based on a spatially averaged and temporally integrated noise index. The optimized trajectory was compared to the standard 6[deg] approach trajectory and also one inspired on fixed wing aircrafts using ILS, so a 3[deg] descent trajectory. The optimized trajectory was 2-6[dB] less noisy (SEL) and the area of SEL above 80[dB] was considerably reduced.

In the Subsonic Rotary Wing project [7], a multi-objective genetic algorithm was used in a procedure developed to identify quiet rotorcraft approach trajectories. This procedure intended to create approach paths that are acceptable to both pilots/passengers and are compared to the standard 6[deg] approach path. One of the two demonstration cases used an acoustic database based on experimental flight tests while the other used a numerically calculated acoustic database. The optimization process used 14 design variables: initial altitude and speed, percentage change in speed and descent rate (based on discrete glide slope options calculated outside the optimization process). The optimization process objective was to optimize the SEL (SELA in the document) over a set of 5 microphones bearing in mind that the path was valid (descent rate constrains). In the case with the experimental database, the SEL was reduced 1-4[dBA] over most parts of the footprint while the one with the numerical database was able to reduce the SEL by an average of 3.2[dBA] of the 5 on-ground microphones. It was found that it's more effective to optimize the rate-of-descent rather than the microphone-helicopter distance.

NUMERICAL OPTIMIZATION PROCEDURE

In this work the acoustic database is numerically pre-calculated, in the form of hemispheres below the rotorcraft, using a comprehensive aeroacoustic chain. The typical AgustaWestland aeroacoustic chain is depicted in Figure 1, but for this optimization work this chain was changed and the optimization block (which now includes the on-ground propagation tool) is added after the Acoustics Solver as shown in Figure 2. Since the acoustic database is pre-calculated, all the trimming, aerodynamic calculations and hemisphere calculations are done only once before the optimization. This database is then fed to the optimizer which will then analyse different paths by feeding the on-ground propagation tool with the desired path information and associated hemispheres.

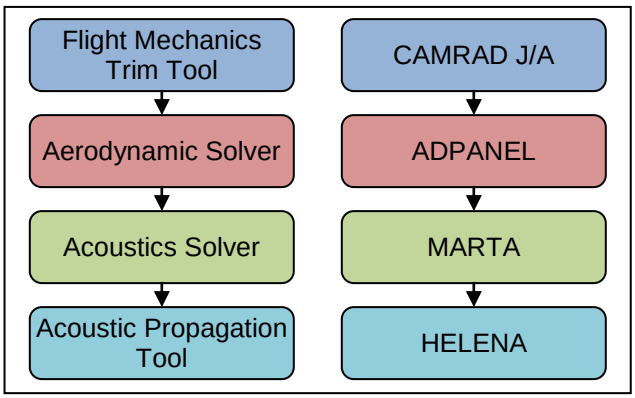

Figure 1 - AgustaWestland aeroacoustic computational chain

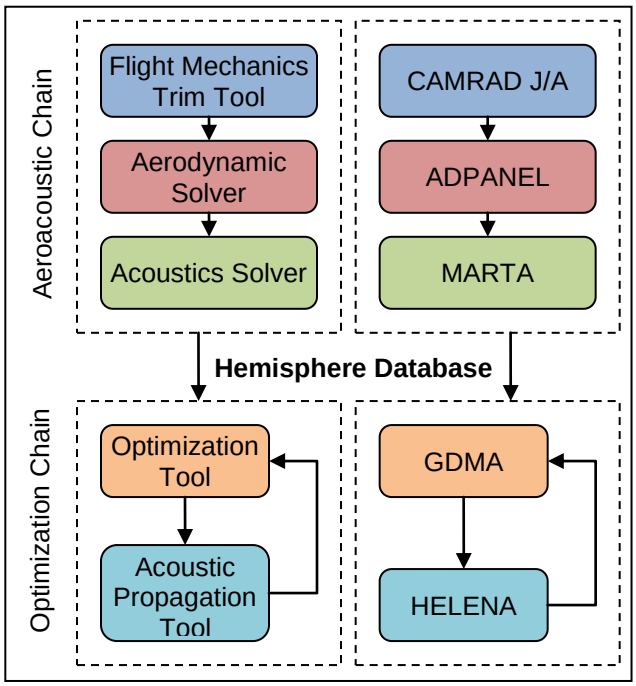

Figure 2 - Modified aeroacoustic-optimization computational chain

Aeroacoustic Chain

To perform aeroacoustic analysis several different tools must be used to correctly calculate the noise footprint on-ground. Referring to Figure 1, the process starts with the flight mechanics trim tool CAMRAD J/A [10] that gives the correct rotor inputs like helicopter pitch angle, collective and cyclic commands and flapping angles to balance the moments and forces in each flight condition. CAMRAD J/A, is a widely used helicopter comprehensive analysis tool. The aerodynamics are based on the blade element model with simplified inflow laws which coupled with a detailed dynamic treatment of the rotor is able to accurately predict the helicopter trim state and rotor blade motion. The trim information is passed on to the aerodynamic solver that accurately calculates the forces on each blade. The aerodynamic solver used in the present optimizations is the in-house solver ADPANEL [8], which is a full-unstructured Multi-Processor panel code coupled with a time-stepping non-linear Free Wake vortex model. This tool implements the most advanced aerodynamic features in the field of potential methods, in particular for the Constant Vorticity Contour (CVC) modelling of both rotary and fixed wing wakes. Thanks to the previous features, ADPANEL is able to analyze in short computational times and with detailed predictions entire helicopter and tiltrotor configurations even operating in ground effect. The wake modelling implemented in ADPANEL is composed of two parts: a “dipole buffer wake sheet”, and a set of “constant vorticity contour vortex filaments”. Buffer wake and CVC vortex filaments are used to represents the vorticity released from rotary and fixed wings for both their components, trailed and shed. The CVC free-wake modelling developed in ADPANEL allows to generate refined roll-ups and high spanwise resolution along rotor blades without enforcing an unnecessary large number of wake elements. Figure 3 shows an example of the computed CVC wake development in case of a full-helicopter configuration operating in OGE. Recent and validated “vortex dissipation laws” have been implemented in ADPANEL in order to represent the increasing of the vortex core with the time passing.

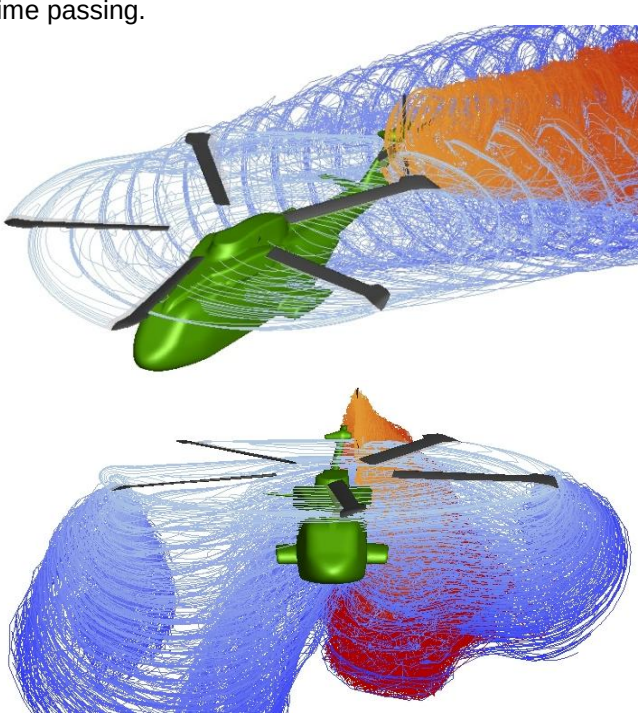

Figure 3 - ADPANEL CVC wake development for a full-rotorcraft configuration operating in OGE.

A lot of the time is spent performing the aerodynamic calculations as the optimum azimuth refinement, necessary to capture the high frequency pressure changes in the blade surface (and high frequency noise), is very fine, in the order of 0.5 to 2[deg]. ADPANEL's advanced features and acceleration methods were essential to reduce the aerodynamic calculations timeframe.

With the blade loading information and rotor/blade geometry it is now possible to calculate the noise footprint on a microphone, be it on the ground or on a hemisphere placed below the rotor. The acoustic tool MARTA, recently developed in AgustaWestland and thoroughly validated against experimental data [9], solves a simplified version of the Ffowcs Williams-Hawkings equation and is used to pre-calculate the noise hemispheres for the defined flight conditions test matrix. MARTA is able to generate the acoustic hemispheres from ADPANEL's aerodynamic and blade geometry data along with CAMRAD's blade motion and helicopter trim data. MARTA is also able to generate sound files, which can be very useful when post-processing the optimization data and subjectively analyse the noise and assess the benefits. In this optimization the aeroacoustic chain is split as the propagation tool HELENA is only used in conjunction with the optimization chain using the hemisphere database calculated by MARTA. HELIcopter Environmental Noise Analysis (HELENA) [11] is common EU software platform for helicopter noise footprint predictions developed under the FRIENDCOPTER EC research program and was compared and validated against AgustaWestland's internal tool HEBETRA [12]. HELENA includes state-of-the-art propagation models and has been demonstrated to accurately predict single-events. The acoustic hemispheres generated by MARTA contain the noise directivity and intensity necessary to optimize for low-noise procedures. A sample hemisphere is shown below in Figure 4.

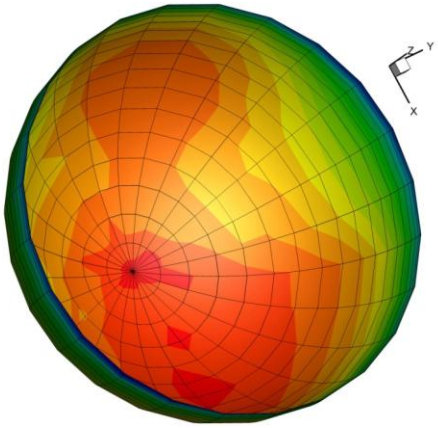

Figure 4 - MR OASPL[dBA]

Optimization Algorithm

The optimization algorithm used in the present work belongs to the family of the Surrogate-Assisted Memetic Algorithms (SAMA). Memetic Algorithms (MAs) are population-based metaheuristic search methods inspired by Darwinian principles of natural evolution and Dawkins notion of a “meme” [13], defined as a unit of cultural evolution that is capable of local refinements [14][15]. The main advantage of MAs over concurrent strategies lies in creating a synergy between global and local search. The global searcher should be able to explore the entire design space, selecting the best solutions in terms of their objective values, while the local searcher should improve further the solutions by means of small local changes in a time-efficient way.

A Genetic Algorithm (GA) is the most appropriate choice as global search algorithm since it is insensitive to local minimum and can easily handle Multi-Objective Optimization Problems (MOOPs). The local search is carried out using a gradient-based algorithm that tries to improve the objective function using a Surrogate Model (SM) of the function itself, generated here by means of a Artificial Neural Network (ANN). This method allows a very efficient local improvement of the individuals coming from a GA population, as the ANN can be evaluated much faster than the original function. The time spent to estimate the local improvements using the ANN is far less than that required for a single flight path simulation. The drawback of this method lies on the approximated nature of the model, but this is overcome by the achievable improvement on convergence rate. The use of an approximated model leads to the so-called surrogate-assisted approach.

GDMA is the selected SAMA algorithm used in present work. It has already been used for rotor blade aerodynamic optimizations [16] and helicopter airfoil multi-objective optimizations [17] with remarkable results. It makes use of the genetic algorithm GDEA [18] as global optimum searcher, the Matlab® *fmincon* [19] gradient-based algorithm for local refinements and the ANN [20] as approximated model. The course of events during a generic optimization procedure is described in Figure 5 and can be summarized as follows: the optimization starts with few GDEA generations, since a minimum number of HELENA’s flight path evaluations are needed to carry out a well approximated ANN’s training. Then, the SAMA framework manages the GDEA to create a new population using the typical genetic evolution operators, but all the new individuals are now locally improved before being evaluated in the actual aeroacoustic chain. The local improvement is driven

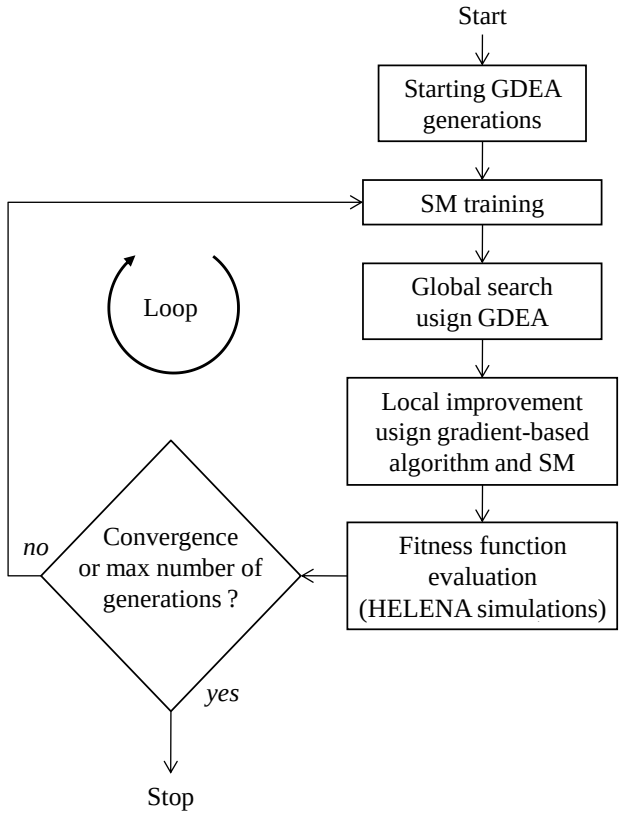

Figure 5 - Schematic representation of the GDMA operation

by the gradient-based algorithm starting from a GDEA's original individual using of the approximated ANN model. The modified (and hopefully improved) population is finally evaluated with HELENA. The process is repeated iteratively until the complete convergence or the attainment of the maximum number of flight path evaluations.

One generic aeroacoustic evaluation is performed by feeding HELENA with the flight path information such as velocity and attitude, noise hemispheres, microphone positions, ground reflection properties and atmospheric propagation parameters. Concerning the hemispheres, since the database is not a continuous one, interpolation is required. This is simply done by choosing the 4 hemispheres, within the whole database, that surround the instantaneous flight condition and doing an inverse distance weighting interpolation. All entire flight path is required to be inside the database's available speed-angle data set, otherwise it is rejected.

PROBLEM SETUP

Database

The aeroacoustic database of both Main and Tail Rotors was initially limited to the typical speed and descent angle combinations. After some preliminary optimizations it was decided that that range should be increased to encompass the speeds from 40 to 100[kts] and descent angles ranging from 0[deg] up to 15[deg]. The speed range was covered with a step of 10[kts] and the angle range with a step of 1[deg] as both were found to provide smooth variations when using the hemisphere inverse distance interpolation scheme mentioned previously. This resulted in 224 aerodynamic and acoustic analysis for both rotors.

Helicopter Description

The helicopter model used in this work is the same described in [21], which is now briefly detailed.

It is a 6500kg machine equipped with articulated MR and TR. The two rotors are oriented such as the MR is rotating counterclockwise (when viewed from above) while the TR is rotating with the advancing side down (ASD), i.e., the TR thrust is pointing starboard. Since the rotors aerodynamic and acoustic analysis is uncoupled, in both calculations the rotors were centered in space ignoring their relative location on the model helicopter as this does not affect the results. The TR is provided with a 15° of cantilever angle which allows the rotor to have not only a side force but also a vertical thrust component. A central center of gravity positioning have been assumed for the calculation of the helicopter trim state for each flight condition. The MR and TR blades have been assumed to be rigid in flap and chord modes and have been equipped with AgustaWestland proprietary airfoils as well as the twist, chord and sweep distributions are taken from proprietary designs. The principal geometric and operating parameters for the MR and TR of the conceptual helicopter are summarized in Table 1.

	Main Rotor	Tail Rotor
Number of Blades	5	4
Rotor Radius	R	R_t=0.2R
Thrust weighted chord	0.064R	0.028R
Angular velocity	Ω	Ω_t=5Ω

Table 1 - Rotors Data

Aerodynamic Modelling

In this work the azimuth refinement was set to 2[deg] as it is enough to capture the high frequency MR BVI noise that characterizes the approach phase. The number of rotor turns was chosen to guarantee a converged near wake solution. The descent angle was found to have little influence on the aerodynamic solution convergence. On the other hand, the speed greatly affects how fast the wake moves away from the rotor and hence the convergence. The 40[kts]

cases required 5 rotor turns to fully converge, the 50[kts] case required 4 rotor turns and the remaining speeds only required 3 rotor turns to achieve convergence. Two wake geometry examples can be found in Figure 6 and Figure 7 for the MR. It's visible that the starting vortex effects are dissipated by the time the rotor reaches the last turn. This was further validated by confirming that the rotor Thrust Coefficient C_T was converged. The MR and TR blades have been modelled using 30 panels in radial direction and a total of 60 panels chordwise (30 on the upper and 30 on the lower surface) in order to properly catch wake induced load fluctuations.

In this work it was assumed that the flight paths will be approximated by quasi-steady manoeuvres, i.e. the unsteady effects of increasing/decreasing the descent angle or decelerating the helicopter will be ignored. This assumption is based on the fact that real approach procedures are characterized by having low accelerations and smooth descent angle variations which have a small effect on the flow field on the rotors. Consequently all the points in the database are steady-state manoeuvres.

According to ICAO rules for acoustic certification tests, ISA+10 atmospheric conditions have been assumed.

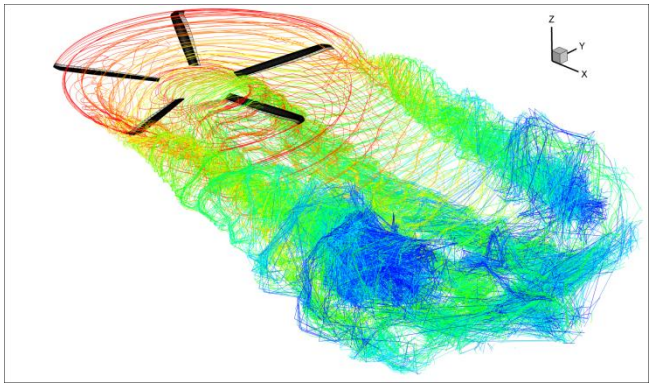

Figure 6 - MR Wake for 40[kts] and 6[deg] descent angle

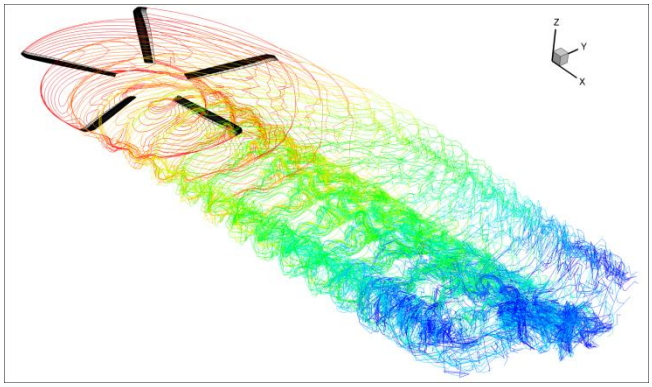

Figure 7 - MR Wake for 100[kts] and 6[deg] descent angle

Hemispheres

The hemispheres created by MARTA for HELENA have a radius of 150[m] and 25 microphones in the longitude direction, with a constant step of 15[deg], and 19 microphones in the latitude direction with a variable step. This was done to optimize the hemisphere discretization so that it captures well the noise gradient close to the hemisphere "equator". The hemispheres were also done using 1/3 Octave Bands (ranging from 50[hz] up to 10000[hz]) instead of rotor tones, as it was found to provide more reliable results.

On-Ground Propagation

HELENA is able to automatically manage both MR and TR hemisphere performing a band sum. Spherical spreading, Doppler shift, atmospheric attenuation, and ground reflection effects are taken into account when propagating on-ground. SAE ARP866A and Nau-Soroka models have been used respectively for atmospheric and ground effects. Ground has been assumed to be made of grass as a typical airfield. This choice influences the value used for the ground resistivity required by the model. Moreover, microphones have been located at 1.2m above the ground. The overhead passage time-histories are evaluated every 0.5s.

LANDING TRAJECTORY OPTIMIZATION

The baseline trajectory, to which all optimized trajectories will be compared to, is depicted in Figure 8. This is a simple trajectory with a constant 6[deg] descent angle, inspired in the approach certification condition.

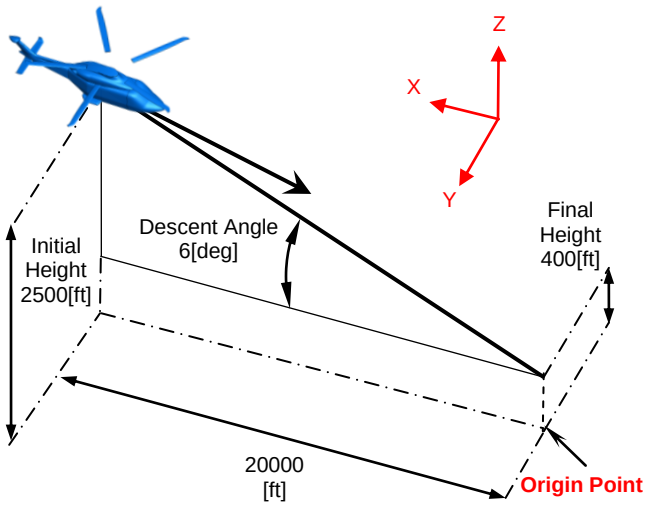

Figure 8 - Baseline Path

The starting velocity was set to 80[kts] and is keep constant for 10000[ft] after which it starts to decrease

linearly up to the final path point where it is 40[kts] and at an altitude of 400[ft]. The point on the ground just below the final path point was set as the coordinate system origin so the path effectively starts at 20000[ft] in the X-direction.Since the aim of this work is to reduce the on-ground noise footprint, four optimizations with different parameters were performed in order to assess which approach is more effective. After each optimization, the best solutions were compared to the baseline and the relative gains assessed.

The parameterization of the flight path was made using b-spline curves [22]. It means that the necessary information to fully describe the helicopter trajectory and attitude were defined by several b-spline control points equally spaced along the X-direction of the path. 5 points were used to describe the Z coordinate of the trajectory and 5 points for the velocity profile. These two parameters are sufficient to completely describe the helicopter descent flight. All the optimizations have the same speed and altitude constrains given by Figure 9.

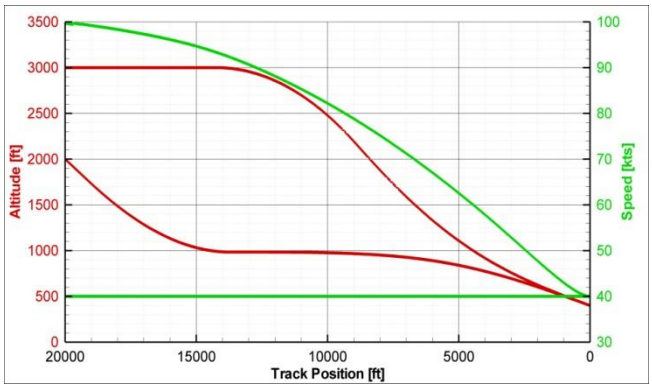

Figure 9 - Path Optimization constrains

The *first optimization* was done to understand how the acoustic parameters SEL and OASPL are related to each other and which one is more effective to minimize the on-ground noise footprint. Both acoustic parameters were evaluated at Microphone1 location (see Figure 10). The *second optimization* was a mono-objective optimization, with SEL being again evaluated at Microphone1 location. This was done to understand if further SEL gains could be achieved by just optimizing for it. The *third optimization* now focus on reducing the SEL at Microphone1 and Microphone2 locations while the *fourth optimization* uses a grid of microphones, Grid1 and Grid2, were the SEL is averaged over them. These microphone grids have their centres coincident with Microphone1 and Microphone2, respectively, and are 2000[ft] long (X-direction) across and 6000[ft] across (Y-direction). The microphones are separated 500[ft] in both directions so there are 5 microphones in the X-direction and 13 microphones in the Y-direction for a total of 65 microphones per grid.

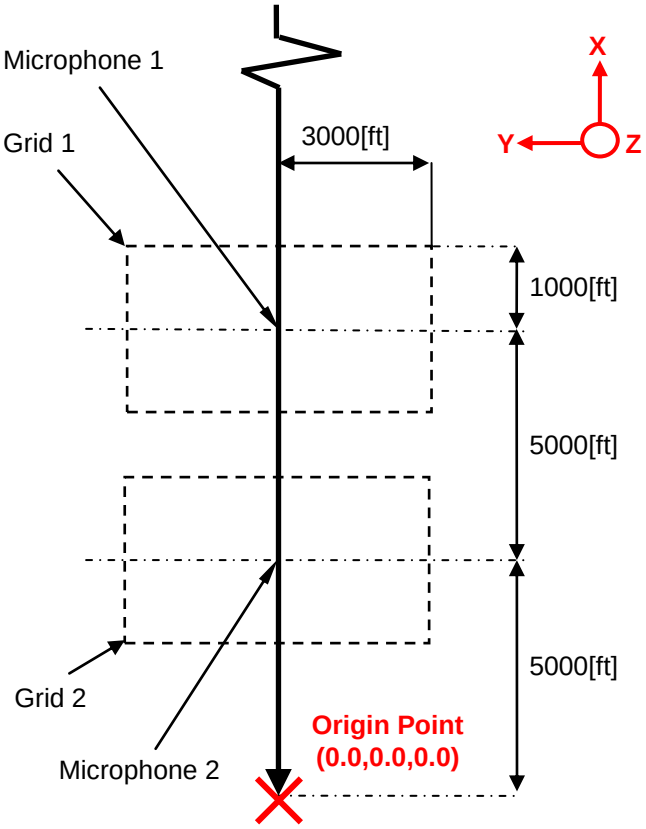

Figure 10 - Microphones and Grids location

Single Point Optimization Results

Optimization1 was focused on studying in one microphone (Microphone1 located at 10000[ft]) how SEL and the peak OASPL (A-Weighted or in [dBA]) relate to each other. The on-ground footprint is evaluated using SEL which is the A-weighted acoustic energy averaged over a period of time. It was developed to provide a means of measuring both the duration and the sound level associated with a particular time period or event after subjective noise studies concluded that longer durations noises to be more annoying than shorter ones [23].

In Figure 11 are the Pareto Front results for Optimization1 against the Baseline trajectory and it's clear that in Microphone1 big gains can be achieved both in terms of peak OASPL and SEL. The maximum reduction in OASPL is 7[dBA] and 5[dBA] in the SEL. This optimization was run for 60 generations but 30 would have been enough to obtain similar results.

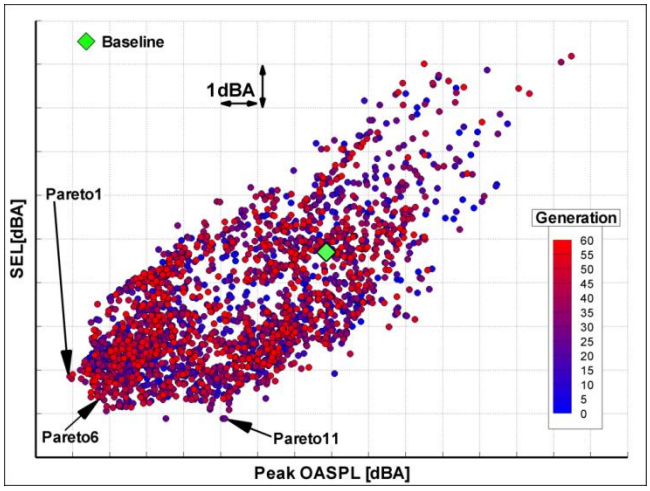

Figure 11 - Optimization 1 solutions

A comparison of the SEL footprint of the Baseline path and 3 of the Pareto Front solutions is found in Figure 12 to Figure 14. The Pareto1 solutions is the best in terms of peak OASPL reduction while Pareto11 is the best one in terms of SEL reduction (at Microphone1 location). From these pictures it's clear that Pareto6 (the compromise solution) is the best solution in terms of reducing the noise footprint if we look at the benefit plots. These plots show the SEL reduction of the optimized paths compared to the Baseline path. From these pictures it is also clear that close to the landing point only small gains can be expected, especially because the trajectory is very constrained close to it.

To understand what is really happening during the path, a plot of the OASPL in 3 different microphones for the 3 Pareto solutions will be compared to the Baseline. These 3 microphones are located at 10000[ft] with Mic1 being located on the right side of Microphone1, 900[ft] away in the positive Y-direction. Mic2 is coincident with Microphone1 and Mic3 is on the left of Microphone1, 900[ft] in the negative Y-direction. These microphones are depicted in all the footprint plots as being the 3 dots at the 10000[ft] mark. The plots in Figure 15 to Figure 17 show that all the Pareto solutions peaks are lower than the Baseline path and that from Pareto1 to Pareto11 the peak OASPL increases. Pareto11 has a smaller area below the OASPL curve, which explains why the SEL is lower even if the OASPL peak is slightly higher.

At this point it's clear that minimizing peak OASPL does not mean that the SEL will be reduced as well. In fact, the smallest footprint was from a path that was a compromise between reducing both acoustic parameters. Further studies (similar to Optimization3/4 but using peak OAPSL instead of SEL) showed that it was more effective to use SEL as the acoustic optimization parameter.

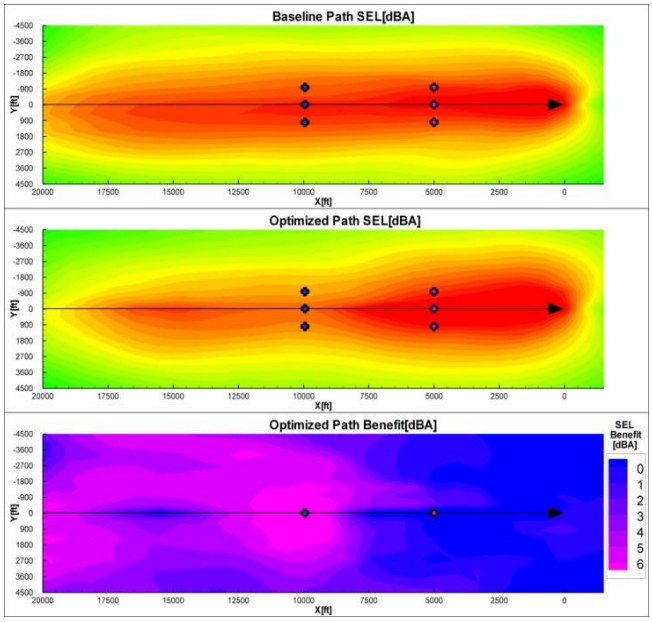

Figure 12 - Pareto1 SEL footprint vs. Baseline footprint

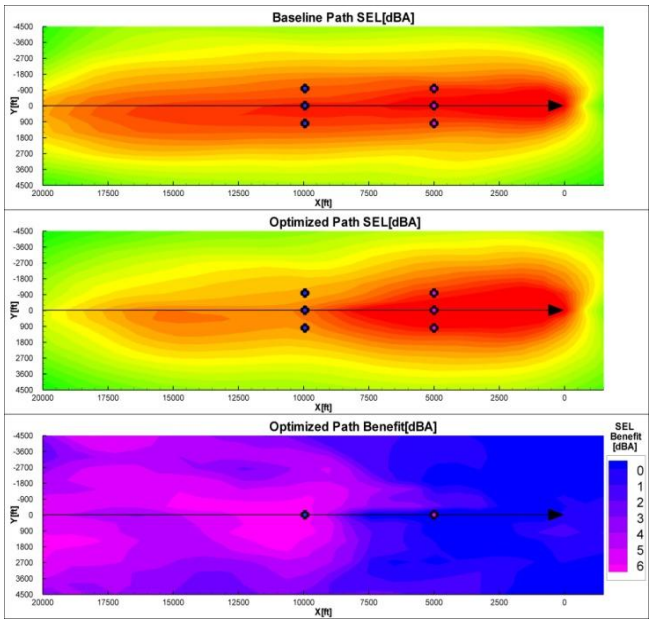

Figure 13 - Pareto6 SEL footprint vs. Baseline footprint

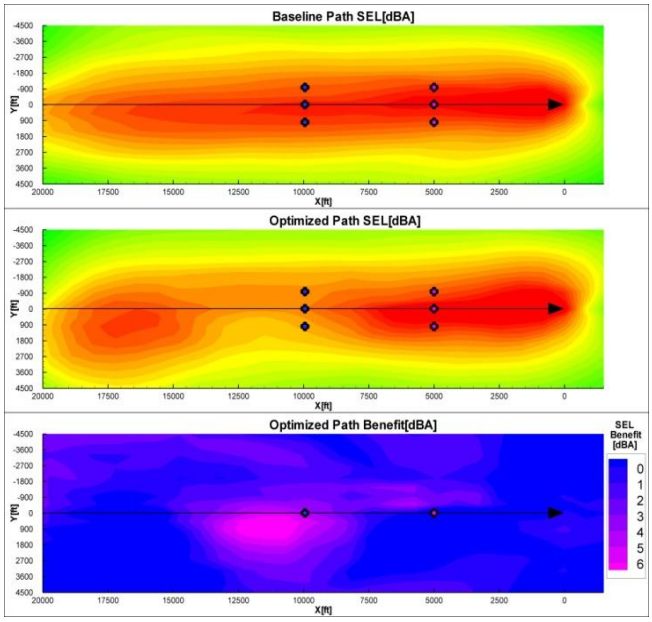

Figure 14 - Pareto11 SEL footprint vs. Baseline footprint

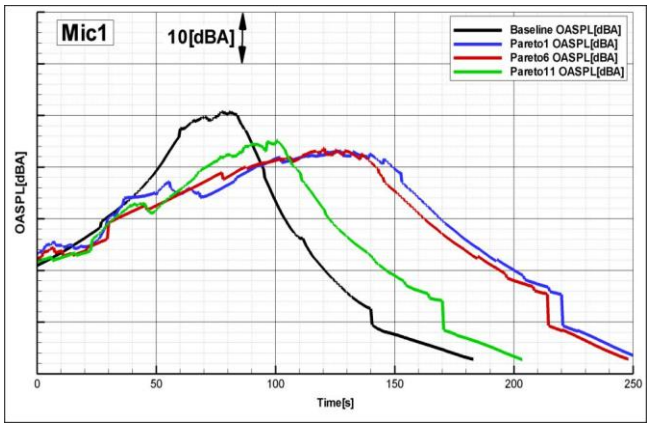

Figure 15 - Pareto1, Pareto6 and Pareto11 OASPL versus the baseline for Mic1

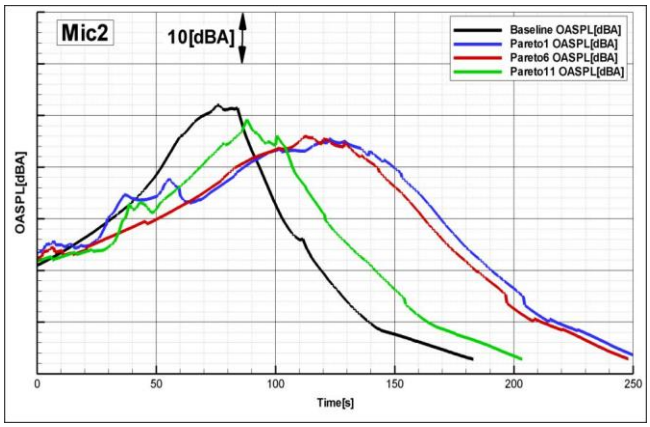

Figure 16 - Pareto1, Pareto6 and Pareto11 OASPL versus the baseline for Mic2

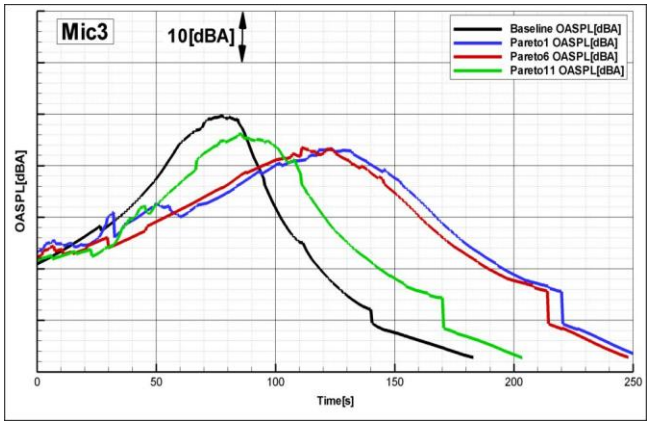

Figure 17 - Pareto1, Pareto6 and Pareto11 OASPL versus the baseline for Mic3

In Optimization2, a mono-objective SEL optimization was done to understand if focusing in just one objective the solution for SEL improves.
The solutions are plotted in Figure 18 and the gain in SEL is the same as in Optimization1. Additionally the SEL footprint (not shown) is very similar so in Optimization1 the optimizer was not influenced by having to search solutions that also minimize the peak OASPL. The opposite is expected, i.e. if the objective was minimizing the peak OASPL then the maximum improvement would be similar to the improvement in Optimization1.

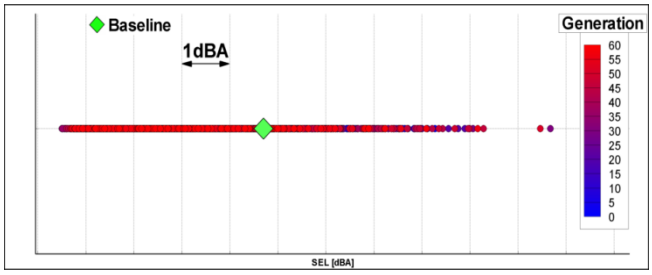

Figure 18 - Optimization 2 solutions

Multi Point/Grid Optimization Results

The last 2 optimizations, Optimization3 and Optimization4, were done to assess if using a grid of microphones instead of a single microphone is beneficial in terms of reducing the on-ground noise footprint. As it turns out using a grid is more effective because just using Microphone1 and Microphone2 the noise is only effectively reduced at those two locations (but the footprint gets worse elsewhere). By instead using Grid1 and Grid2 the SEL is not only reduced at those points but also the on-ground noise footprint is reduced. The solutions of Optimization4 are shown in Figure 19 and as expected it's possible to obtain more improvements in Grid1 than in Grid2, mainly due to the fact that the end of the path is more constrained.

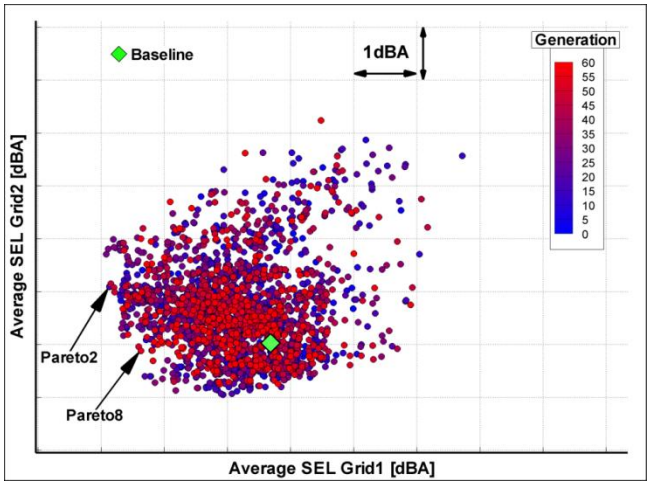

Figure 19 - Optimization 4 solutions

The paths of Pareto2 and Pareto8 of Optimization4 will now be compared between them in terms of path information and with the Baseline path in terms of footprint. The path information shown in Figure 20 and Figure 21 for both Pareto paths shows that the main difference between them is the starting altitude, as Pareto2 starts 300[ft] higher and the fact that to compensate that extra altitude the maximum descent angle is higher. Pareto8 path is also smother and the maximum velocity is lower. These trajectories seem acceptable, especially since they don't have any abrupt velocity and descent angle changes and also because the Rate of Descent Ratio R is kept below 1, as can be seen in Figure 24 and Figure 25. This parameter is often used as a rule of thumb to describe pilot acceptance [7] and is calculated by dividing the Rate of Descent in [ft/min] by the altitude in [ft]. The rule states that R should be kept lower than 1 and this is respected by both paths.

The on-ground noise footprint of Pareto8 is overall better, specially on the left side of the trajectory (Figure 22 versus Figure 23). The OASPL comparison (Figure 26 to Figure 31), which now also includes the 3 other microphones, Mic4 to Mic6 (similar to Mic1 to Mic3 but located at the 5000[ft] mark) shows that apart from Mic5 (coincident with Microphone2 and located at X=5000[ft] and Y=0[ft]) shown in Figure 30 all the other ones have the OASPL peak reduced by around 5[dBA]. The slightly higher peak in OASPL in Mic5 reveals that although the overall footprint is reduced, it is very difficult to optimize the noise below the helicopter trajectory close to the landing point as the landing point constrains influence the path well before. The overall footprint is reduced as the 2 side microphones, Mic4 and Mic6, have a lower SEL, mainly due to the fact that the peak OASPL is lower. Since in both paths the velocity is in general lower than the baseline, the OASPL curves are more stretched.

Comparing Optimization4 and Optimization1 results, the footprint actually seems to increase, especially on the left side of the track. This is because by trying to improve the Grid2 area, the noise closer to the landing point will effectively be reduced but the region before it is also negatively affected.

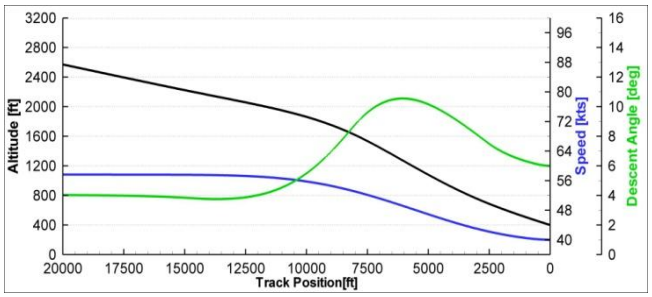

Figure 20 - Pareto2 path information

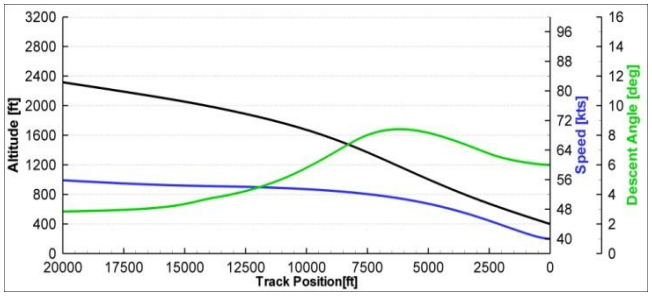

Figure 21 - Pareto8 path information

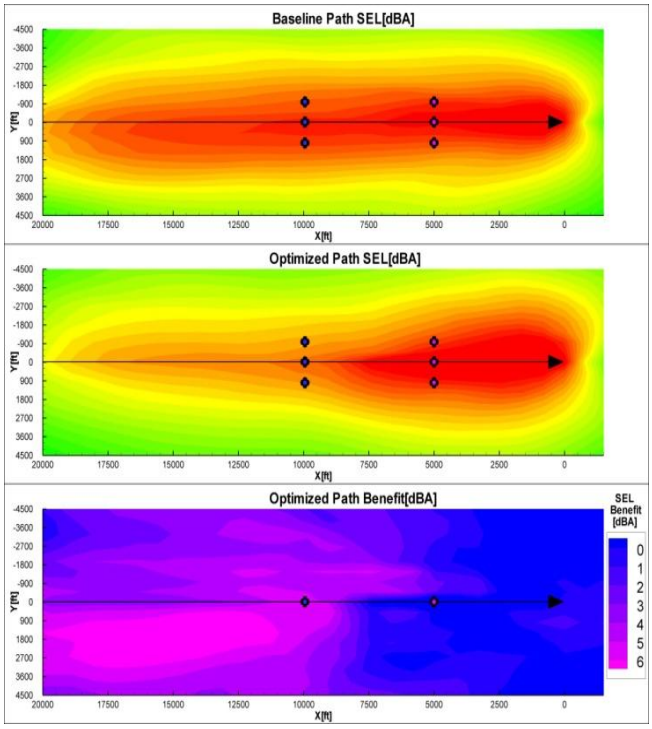

Figure 22 - Pareto2 SEL footprint vs. Baseline footprint

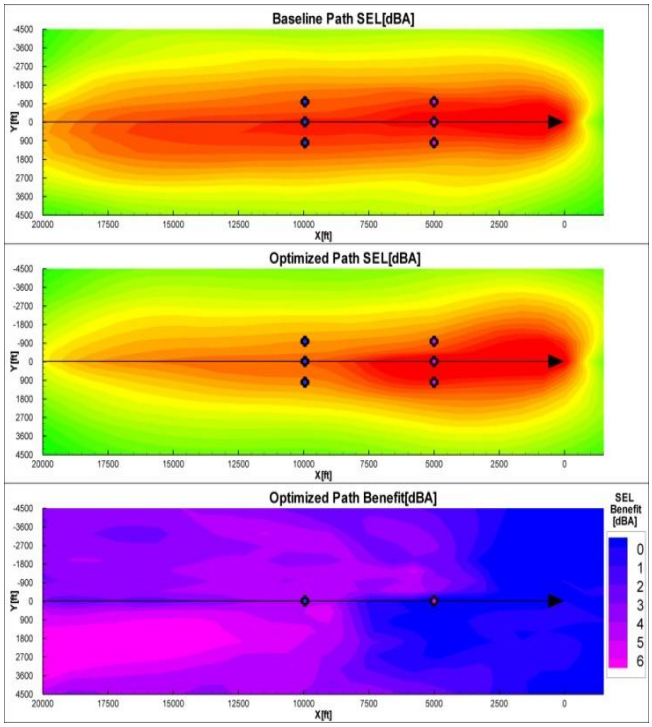

Figure 23 - Pareto8 SEL footprint vs. Baseline footprint

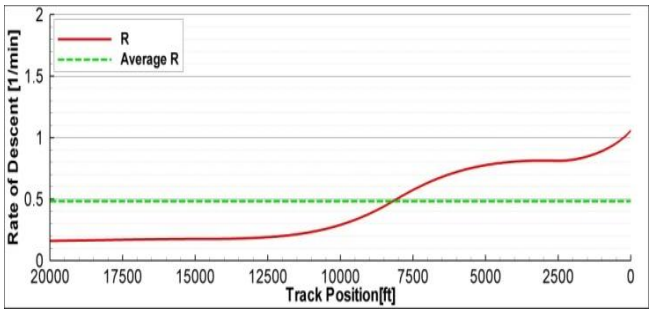

Figure 24 - Pareto2 Rate of Descent Ratio variation along the path

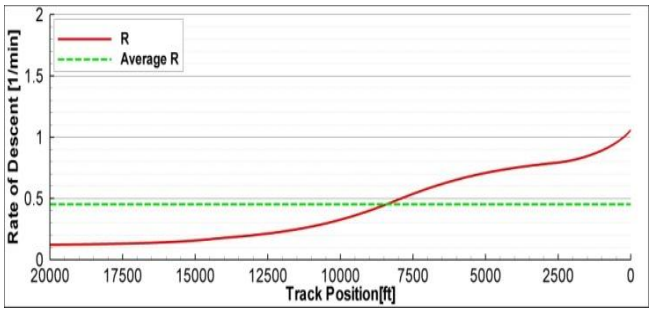

Figure 25 - Pareto8 Rate of Descent Ratio variation along the path

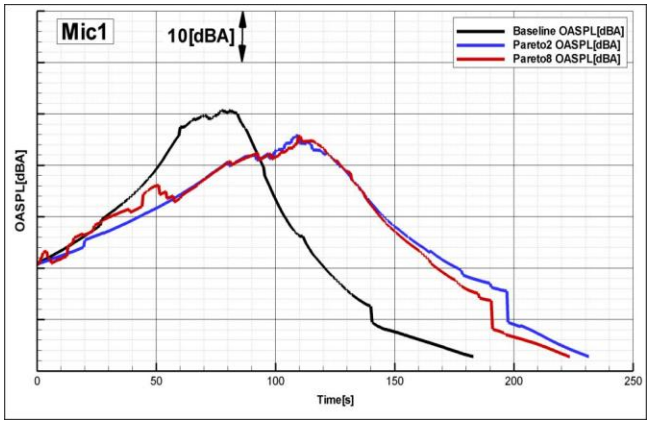

Figure 26 - Pareto2 and Pareto3 OASPL versus the baseline for Mic1

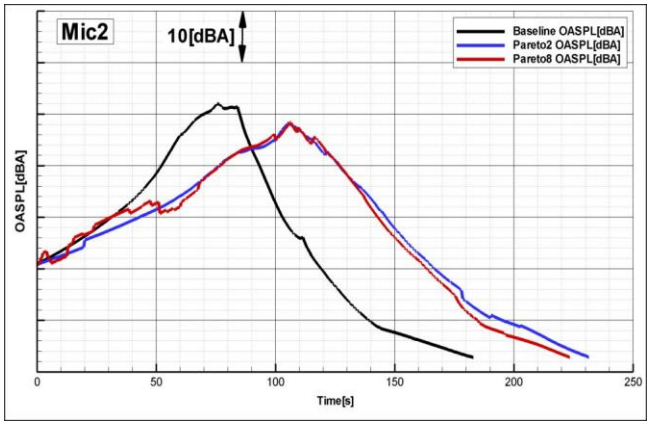

Figure 27 - Pareto2 and Pareto3 OASPL versus the baseline for Mic2

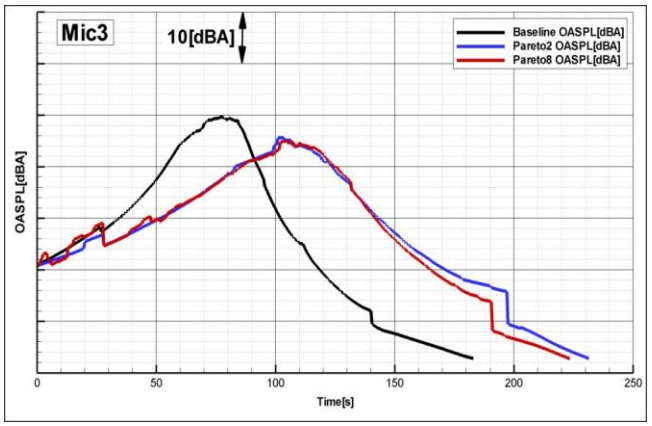

Figure 28 - Pareto2 and Pareto3 OASPL versus the baseline for Mic3

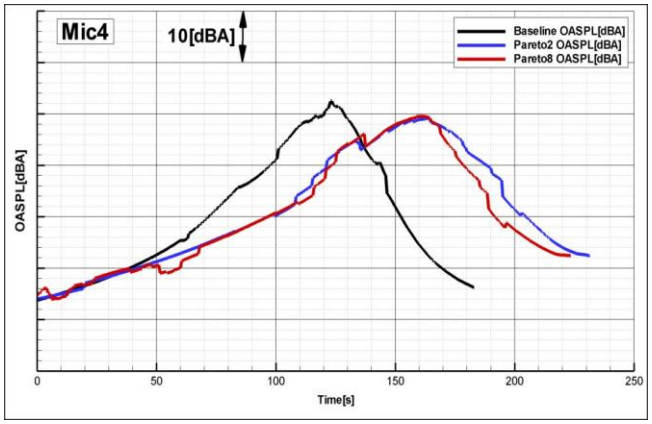

Figure 29 - Pareto2 and Pareto3 OASPL versus the baseline for Mic4

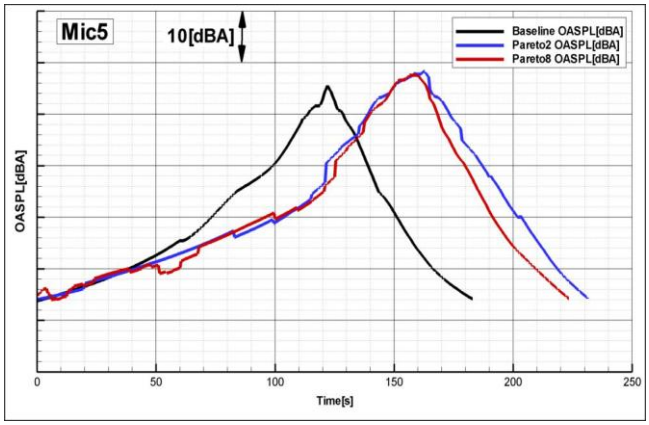

Figure 30 - Pareto2 and Pareto3 OASPL versus the baseline for Mic5

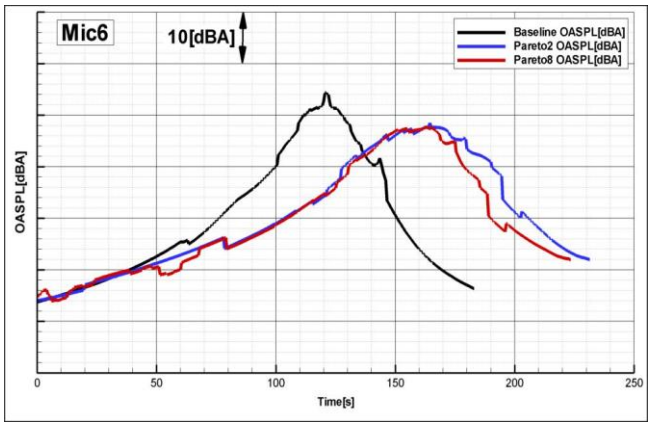

Figure 31 - Pareto2 and Pareto3 OASPL versus the baseline for Mic6

CONCLUSIONS AND FUTURE WORK

Optimizing helicopter flight paths for low noise is a very challenging task as aeroacoustics are a highly non-linear phenomena and involve coupling many tools. With this in mind, a very straightforward, robust and fast optimization strategy was developed that can analyse any type of rotorcraft. With this strategy it was possible to decrease the helicopter noise before the landing point by as much as 5[dBA] in SEL and also decrease the peak OASPL by around 5[dBA] in the microphone locations analysed. From the different studies it was found that the optimizer was very effective at reducing noise at punctual locations but that resulted in increased on-ground noise footprints. To avoid this the punctual microphones were replaced with an array of microphones surrounding that point and this way it was possible to both decrease the noise locally and the on-ground footprint.

Since the Main Rotor tonal noise is dominant during the approach/landing phase, it's expected that the improvements found in this work will be reflected in real flight paths.

The current optimization procedure assumes that between each path point the accelerations don't affect the flow field on the rotor and the noise produced by it. Some studies have developed a formula to account for the accelerations as a correction to the descent angle. We intend to test these corrections and, if valid in our model, include them for more accurate noise predictions. Additionally we intend to replace one of the acoustic objectives with one aeromechanics objective, one that minimizes pilot effort and increases passenger comfort, possibly based on the Rate of Descent Ratio. Finally we intend to focus on other rotorcraft configurations, like the tilt-rotor, which will require a more efficient database preparation and optimization procedure to cope with the increased complexity of the problem.

ACKNOWLEDGEMENTS

This research activity is partially funded by the Clean Sky Joint Undertaking under projects GAM-GRC, related to activities performed within the ITD Green Rotorcraft. The authors would like to thank Dr. Sebastian Dubois of the Clean Sky Joint Undertaking for the management monitoring of the program.

REFERENCES

[1] Le Duc A., Spiegel P., Guntzer F., Lummer M., Gotz J., "Modelling of Helicopter Noise in Arbitrary Maneuvre Flight using Aerocoustic Database" Institute of Aerodynamics and Flow Technology, Technical Acoustics Division

[2] Spiegel P., Guntzer F., Le Duc A., Buchholz H., "Aeroacoustic Flight Test Data Analysis and Guidelines for Noise-Abatement-Procedure Design and Piloting", 34th European Rotorcraft Forum, 16-19 September 2008, Liverpool, UK

[3] Guntzer F., Spiegel P., Lummer M., "Genetic Optimizations of EC135 Noise Abatement Flight Procedures Using an Aeroacoustic Database", 35th European Rotorcraft Forum, 22-25 September 2009, Hamburg, Germany

[4] Perez G., Costes M., "A New Aerodynamic & Acoustic Computation Chain for BVI Noise Prediction in Unsteady Flight Conditions", American Helicopter Society 60th Annual Forum, 8-10 June 2004, Baltimore, USA

[5] Ikaida H., Tsuchiya T., Ishii H., Gomi H., Okuno Y., "Numerical Simulation of Rela-Time Trajectory Optimization for Helicopter Noise Abatement", Journal of Mechanical Systems for Transportation and Logistics, Vol. 3, No. 2, 2010

[6] Ikaida H., Tsuchiya T., Ishii H., Gomi H., Okuno Y., "Real-Time Trajectory Optimization for Noise Abatement of Helicopter Landings", Journal of Mechanical Systems for Transportation and Logistics, Vol. 4, No. 2, 2011

[7] Padula L., Burley L., Boyd D., Marcolini A., "Design of Quiet Rotorcraft Approach Trajectories", NASA/TM-2009-215771, Langley Research Center, Hampton, Virginia, June 2009

[8] D'Andrea A., "Development of a Multi-Processor Unstructured Panel Code coupled with a CVC Free Wake Model for Advanced Analysis of Rotorcraft and Tiltrotors", AHS 64th Annual Forum, Montréal, Canada 2008

[9] Cruz L., "Comparison Between MARTA Aeroacoustic Tool and Experimental Data - Application to the AW139 Helicopter", AgustaWestland Internal Report, Issue A, September 2011

[10] Johnson, W., "Camrad/JA - A Comprehensive Analytical Model of Rotorcraft Aerodynamics and Dynamics - Volume II: User's Manual", Johnson Aeronautics, 1988

[11] Tuinstra M., Duque Geraldes C.M.,"HELicopter Environmental Noise Analysis (HELENA) Software Tool", NLR-CR-2010-346

[12] Melone S., " HELIcopter Environmental Noise Analysis (HELENA) Software Tool Validation", AgustaWestland Internal Report, Issue A, January 2011

[13] Dawkins, R, "The Selfish Gene", New York City, Oxford University Press, 1976

[14] Lim, D., Jin, Y., Ong, Y. S., Sendhoff, B., "Generalizing Surrogate-Assisted Evolutionary Computation," IEEE Transactions on Evolutionary Computation, Vol. 14, No. 3, 2010, pp. 329-355

[15] Krasnogor, N., Ishibuchi, H., "IEEE Transactions on Systems, Man and Cybernetics - Part B: Special Issue on Memetic Algorithms," Vol. 37, No. 1, February 2007

[16] Massaro A., D'Andrea A., Benini E., "Multiobjective-Multipoint Rotor Blade Optimization in Forward Flight Conditions Using Surrogate-Assisted Memetic Algorithms", 37th European Rotorcraft Forum, September 13th – 15th, 2011, Gallarate, Italy

[17] Massaro A., Benini E., "Multi-Objective Optimization of Helicopter Airfoils Using Surrogate-Assisted Memetic Algorithms", Journal of Aircraft, Vol. 49, No. 2, pp. 375-383, March–April 2012,

[18] Toffolo A., Benini E., "Genetic Diversity as an Objective in Multi-Objective Evolutionary Algorithms", Evolutionary Computation, Massachusetts Institute of Technology, Vol. 11, No. 2, pp. 151-167, 2003

[19] The Mathworks, "Matlab R2009a Guide".

[20] Schmid, M. D., "A neural network package for Octave - User's Guide - Version: 0.1.9.1", 2009

[21] Melone S., D'Andrea A., "Helicopter Main Rotor - Tail Rotor Interactional Aerodynamics and Related Effects on the On-Ground Noise Footprint", 37th European Rotorcraft Forum, September 13th – 15th, 2011, Gallarate, Italy

[22] Rogers, D. F., "An Introduction to NURBS With Historical Perspective", Elsevier, 2001

[23] Bolt Beranek and Newmen Inc.,"Handbook of Aircraft Noise Metrics", U.S. Department of Commerce, National Technical Information Service N81-21871, Canoga Park, CA, 1981